HHS Public Access

Author manuscript

J Immunol. Author manuscript; available in PMC 2019 November 15.

Published in final edited form as:

J Immunol. 2018 November 15; 201(10): 2899–2909. doi:10.4049/jimmunol.1800254.

Vasodilator Stimulated Phosphoprotein (VASP) Regulates Natural Killer Cell Lytic Granule Convergence

Katelynn M. Wilton[*,†] and **Daniel D. Billadeau**[*,‡]

[*] Department of Immunology, Schulze Center for Novel Therapeutics, College of Medicine, Mayo Clinic, Rochester, MN 55905

[†] Medical Scientist Training Program, Schulze Center for Novel Therapeutics, College of Medicine, Mayo Clinic, Rochester, MN 55905

[‡] Division of Oncology, Schulze Center for Novel Therapeutics, College of Medicine, Mayo Clinic, Rochester, MN 55905

Abstract

Natural killer (NK) cells eliminate viral-infected and malignant cells through a highly orchestrated series of cytoskeletal rearrangements, resulting in the release of cytolytic granule contents toward the target cell. Central to this process is the convergence of cytolytic granules to a common point, the microtubule-organizing center (MTOC), before delivery to the synapse. In this study, we show that Vasodilator Stimulated Phosphoprotein (VASP), an actin regulatory protein, localizes to the cytolytic synapse, but surprisingly shows no impact on conjugate formation or synaptic actin accumulation despite being required for human NK cell-mediated killing. Interestingly, we also find that a pool of VASP co-purifies with lytic granules and localizes with lytic granules at the MTOC. Significantly, depletion of VASP decreased lytic granule convergence without impacting MTOC polarization. Using the KHYG-1 cell line in which lytic granules are in a constitutively converged state, we find that either VASP depletion or F-actin destabilization promoted spreading of formerly converged granules. Our results demonstrate a novel requirement for VASP and actin polymerization in maintaining lytic granule convergence during NK cell-mediated killing.

Introduction

Natural killer (NK) cells are innate lymphocytes that can kill viral-infected, stressed and cancer cells through the secretion of preformed lytic granules. This process is dependent on multiple external signals from the target cell, which are transferred by activating, inhibitory and co-receptors on the NK cell surface (1–4). Both the decision process and the act of cytolysis are highly regulated and dependent on the actin and microtubule cytoskeletons (5, 6). For example, F-actin accumulation at the cytolytic synapse formed between the NK cell and target cell facilitates and increases integrin-mediated adhesion. Significantly,

Correspondence: Daniel D. Billadeau, Division of Oncology Research and Schulze Center for Novel Therapeutics, College of Medicine, Mayo Clinic, 200 First Street SW, Rochester, MN, 55905, USA; billadeau.daniel@mayo.edu; Phone: (507) 266-4334; Fax: (507) 266-5146.

Disclosures

The authors have no financial conflicts of interest.

inactivating mutations in genes encoding regulators of F-actin generation such as DOCK8 and WASP, result in primary immunodeficiencies that impact not only F-actin accumulation at the cytolytic synapse, but also integrin-mediated adhesion, and ultimately NK cell lytic potential. In addition to the actin cytoskeleton, the microtubule cytoskeleton is engaged downstream of activating receptors. In fact, during the process of NK activation, lytic granules undergo microtubule minus-end directed movement ultimately converging around the microtubule-organizing center (MTOC)(7). Simultaneously, the MTOC polarizes toward the NK-target cell interface, thereby delivering its lethal payload to the appropriate cellular location. The entirety of this process is dependent on the extremely delicate and precise movement of cytoskeletal structures, most notably tubulin and actin. Despite this importance, the roles of many molecular cytoskeletal regulators in this process have not yet been ascertained.

One such molecular regulator, vasodialator stimulated phosphoprotein (VASP), regulates actin polymerization in various cell types (8–21). VASP is a member of the Ena/VASP family of actin regulatory proteins, which contain a conserved EVH1 domain, largely thought to regulate location through binding partners, a central proline rich region, and a distal conserved EVH2 domain, which allows tetramerization and actin binding (22). Generally, VASP has an anti-capping activity, which promotes the polymerization of F-actin in a linear, non-branching fashion (9, 23–25). VASP is also believed to contribute to actin polymerization through its binding interactions within the EVH2 domain, which allow it to interact with globular and filamentous actin in close proximity, potentially catalyzing the further polymerization of actin (22, 26). Interestingly, VASP is known to signal via inside out signaling to activate integrins (27), including LFA-1, which is essential for formation of tight conjugates between immune cells including NK – target cell interaction (28–30) and downstream cytoskeletal movement, including MTOC polarization and lytic granule convergence (31, 32). Within immune cells, VASP has been implicated in cell-cell adhesion (33), the movement of immune cells into tissues (diapedesis) (34) and the general accumulation of F-actin after T cell activation (35). Though there are some obvious NK cell corollaries with the above processes (NK cell movement and conjugate formation), the role of VASP in NK cells remains unknown.

In this study, we describe a novel role for VASP in NK cells. VASP knockdown inhibits NK cell cytotoxicity, without impacting integrin- or F-actin-dependent conjugate formation. Instead, we found that VASP is required for the maintenance of lytic granule convergence at the MTOC and uniquely aids actin accumulation at cytolytic granules. In addition, our data highlight a previously unappreciated role for F-actin in the maintenance of lytic granule convergence to the MTOC.

Materials and Methods

Cells, reagents and Antibodies

All cells were maintained in standard RPMI with 10% Fetal Bovine Serum (Sigma or Atlanta Biologicals), Penicillin-Streptomyocin (Corning), with or without additional supplements, including Sodium Pyruvate (Corning), MEM non-essential amino acids (Corning), Glutamine (Corning) and recombinant human IL-2 (Peprotech). YTS cells were

obtained from Dr. E. Long (NIH, Bethesda, MD), NKL cells from Dr. M. Robertson (Indiana University Cancer Center, Indianapolis, IN), and KHYG-1 cells from Leibniz Institute DSMZ. 721.221 and K562 cells were obtained from the ATCC. Primary human NK cells were extracted from peripheral blood products using Ficoll-Hypaque (GE Healthcare) and the Rosette Separation NK cell isolation kit (Stem Cell Technologies) using a modified protocol (36). In brief, peripheral blood mononuclear cells (PBMCs) were isolated through centrifugation and layering. Total PBMCs were then mixed with red blood cells at a ratio of 1:100 and Rosette Separation antibody cocktail was added and incubated for 20 minutes at room temperature. Ficoll-Hypaque-mediated separation was repeated and the resulting cells were analyzed for purity by flow cytometry using FITC, PE, Percp and APC conjugates antibodies against CD4, CD8, CD3 and CD56 (BD Biosciences). Rabbit polyclonal antisera to VASP, and WASP were previously described (37, 38). Antibodies to β-actin, γ-tubulin and talin were obtained from Sigma (St. Louis, Missouri). Anti-GAPDH antibody was obtained from Genetex (Irvine, CA), anti-CD107a/LAMP-1 (for immunofluorescence from Abcam (Cambridge, MA), anti-Perforin from BD Pharmingen (San Diego, CA), anti-α-Tubulin from Invitrogen (Carlsbad, CA), anti-NKG2D (for stimulation) and anti-2B4 (for immunofluorescence) from R&D Systems (Minneapolis, MN), anti-α-tubulin from Cell Signaling Technologies (Danver, MA), and anti-Granzyme B from Santa Cruz (Dallas, TX). Monoclonal antibodies to 2B4 (clone C1.7, for stimulation) and CD16 (3G8) were obtained from hybridomas. An additional mouse anti-VASP antibody was obtained from Enzo Life Sciences (Farmingdale, NY). The antibody against LFA-1 / β_2 integrin was clone MHM23. Latrunculin-A was obtained from Sigma.

Small interfering RNA constructs and nucleofection

Small interfering RNA constructs were obtained from Invitrogen and ThermoScientific. Silencing RNAs used included a control siRNA (siCtrl : 5' – UUCUCCGAACGUGUCACGU-3'), and two siRNAs against VASP (A – 5' – UGGCGUUCAUCUCUUCCAUGAGUCC-3', and B – 5' – GCCAAGGAUGAAGUCGUCUUCUUCG – 3'). Nucleofection of siRNA oligos into NKL, primary human NK cells and KHYG-1 was done using the standard protocol and Nucleofection V kit (Lonza) and an Amaxa Nucleofector I as previously described (39, 40). All subsequent assays were completed 48 (primary human NK cell) or 72 hours (NKL and KHYG-1) after nucleofection. All knockdown experiments were verified by immunoblotting for decrease in total VASP protein. A redundant control showing knockdown of VASP by immunofluorescence was done on all imaging experiments that could accommodate the additional fluorescent VASP stain

Cytotoxicity Assay

Chromium (^{51}Cr) release assays were performed as previously described (41, 42). In brief, target 721.221 cells were labelled with ^{51}Cr (Perkin Elmer) and co-cultured with dilutions of NK cell and % cytotoxicity was determined in reference to a standard spontaneous (standard cell culture media) and maximum (0.5% Triton X, Sigma) release. All assays were co-cultured for 3 hours and resulting ^{51}Cr release was measured using Luma-96 plates (Perkin Elmer), Top-Seal A Plus (Perkin Elmer) and Top Count NXT Microplate Scintillation and Luminescence Counter. Primary NK cell reverse antibody-dependent cytotoxicity assays

were completed using antibodies against NKG2D (R&D Systems), 2B4 (C1.7) and CD16 (3G8) and the P815 cell line as previously described (41).

Conjugate and Degranulation Assays

NKL or primary human NK cells were labelled with Calcein-AM (Invitrogen) for 1 hour with intermittent mixing. Target 721.221 cells were stained with 7-amino-4-chloromethylcoumarin (CMAC, Invitrogen) for 30 minutes in serum free media with subsequent washing and incubation in complete media. Labelled cells were washed and resuspended in serum free media at 1.5–3 million cells per mL (NKL and primary human NK cells) and 2.5 million cells per mL (721.221). Cells were incubated on ice for 20 minutes and then mixed together (250μL of each) and centrifuged at 200rpm for 5 minutes at 4°C and then incubated at 37°C for the indicated amount of time. Conjugate formation was terminated by vigorous vortexing and fixation with 4% Paraformaldehyde in phosphate buffered saline (PBS). Conjugate formation was assessed using two –color flow cytometry and analyzed by quantifying the number of target bound NK cells (CMAC+Calcein+) divided by the total number of NK cells (Calcein+).

To assess degranulation, a conjugate assay, as described above, was completed over a longer time course up to one hour. Following the conjugate assay, cells were fixed for a minimum of 30 minutes in 4% paraformaldehyde and then washed and stained for flow cytometry using either APC conjugated anti-LAMP-1 (BD Pharmingen) or an APC conjugated anti-Isotype IgG1 (BD Biosciences). Cells were subsequently washed and evaluated using 3-color flow cytometry for the mean fluorescence intensity of APC on all $CMAC^{+}Calcein^{+}$ conjugates.

Cell microscopy and analysis

Microscopy of single KHYG-1 cells, with or without siRNA nucleofection, were plated onto poly-L-lysine (PLL)-coated coverslips for 15 minutes at 37°C. For Latrunculin-A treatment experiments, KHYG-1 cells were incubated with latrunculin-A (1 μM, Sigma) or DMSO for 10 minutes at 37°C and then resuspended and allowed to adhere to PLL-coated coverslips for an additional 5 minutes. Conjugates of NKL/primary NK cells and 721.221 were made as described above, with 250 μL of 7-amino-4-chloromethylcoumarin (CMAC)-stained 721.221 (2.5 million cells / mL, Invitrogen) mixed with 250 μL of NKL / primary human NK cells (1.5–3 million cells / mL) in serum free media and centrifuged together at 200 rpm for 5 minutes at 4°C. For single time point siRNA experiments, cell mixtures were incubated at 37°C for 15 minutes, resuspended and allowed to adhere to PLL-coated coverslips for an additional 15 minutes at 37°C. For time point experiments, cell mixtures were allowed to incubate at 37°C for 1, 5, 15, and 25 minutes, then resuspended and allowed to adhere to PLL-coated coverslips for 5 minutes at 37°C to result in the indicated times.

Cells were fixed with molecular grade 4% paraformaldehyde in PBS (18 minutes), permeabilized with 0.15% Surfact-Amps (Thermo Scientific) in PBS (3 minutes), blocked with fetal-bovine serum based blocking reagent and stained with the indicated antibodies. Secondary reagents included Alexa Fluor 568, and Alexa Fluor 647 conjugated versions of donkey anti-mouse IgG and donkey anti-rabbit IgG antibodies (Invitrogen). F-actin was

visualized using Alexa Fluor 488 Phalloidin (Invitrogen). Coverslips were mounted onto glass slides using SlowFade (Invitrogen) and examined on an C-Acromat 63x / 1.2w DIC water lens equipped on a LSM-710 laser scanning confocal microscope (Carl Zeiss). Images were captured using the LSM software package (Carl Zeiss).

Cellular Fractionation, Immunoprecipitation and Protein Analysis

Preparation of post nuclear, post mitochondrial, $CaCl_2$ and crude lysosomal fractions were obtained as described previously (42). Briefly, NKL or KHYG-1 cells were suspended 0.25 M sucrose in 10 mM Tris [pH 7.4] appropriate to the number of cells and homogenized using a dounce tissue homogenizer. The resulting homogenate was centrifuged at 600 x g for 5 minutes at 4°C to obtain post nuclear lysate (PNL), which specifically contained all organelles smaller than the nucleus and the general cytoplasmic lysate, but specifically excluded the nuclear material. The resulting supernatant was then spun at 12,000 x g for 10 minutes at 4°C to yield post mitochondrial lysate (PML), which similarly removed the mitochondria while leaving smaller organelles intact. The supernatant was then supplemented with $CaCl_2$ to a final concentration of 8 mM before centrifugation at 14,000 rpm for 15 minutes at 4°C. This allowed for precipitation of the lysosomes and other granules from the general cytoplasmic contents. The resulting supernatant was removed as the non-lysosomal fraction ($CaCl_2$), and represents the general cytoplasmic component and all organelles not removed by the prior treatments. The pellet was washed once in 150 mM KCl in 10 mM Tris [pH 7.4] and resuspended in either 150 mM KCl in 10 mM Tris [pH 7.4] to obtain the crude lysosomal fraction (CLF). This fraction is the subset of the PML containing the larger $CaCl_2$-sensitive organelles, while the $CaCl_2$ fraction contains the rest of the general cytoplasmic protein. All fractions were retained for immunoblot analysis or lysis buffer for immunoprecipitation. Immunoprecipitation was performed as previously described (42, 43) using anti-VASP antibody and protein A sepharose beads (Sigma Chemical). All immunoblot analysis was performed after lysis in 10 mM Tris with 50 mM NaCL, 5 mM EDTA, 50 mM NaF, 30 mM Na4P2O7, and 1% Triton X-100 at pH of 7.4 or in 1 M Hepes (pH 7.2) with 50 mM Potassium Acetate, 1 mM EDTA, 200 mM D-Soribitol and 0.1% Triton X-100. Protease inhibitors (1 mM PMSF, 5 ug/mL aprotinin and 10 ug/mL leupeptin) and 1 mM Sodium Orthovanadate were added to all lysis buffers. For both immunoprecipitation and immunoblot, protein was quantified by Bradford assay for loading, with an excess of protein loaded into all lanes of CLF, as this was necessary for visualization.

Image and Statistical Analysis

Microscopic images were processed and analyzed using ImageJ software (version 1.50i; NIH). Fluorescence quantification was done on unadjusted images, where in many cases the cellular structures were difficult to see by human eye, but would fall in the dynamic range of the software. Manuscript images shown are adjusted using ImageJ to increase clarity and for viewing by the human eye. For all representative images, modifications were consistent within an experiment, with the exception of experiments where an antibody was altered (for example, rIgG versus LAMP-1 versus VASP). To calculate the relative amount of a specific protein (i.e. LFA-1, talin or F-actin) within the cytotoxic synapse (or membrane or perigranular area), the area of the interest and the area of the total NK cell were each

inscribed using a hand-drawn gate guided by Phalloidin staining to indicate cortical F-actin or clustered perforin staining to indicate the position of the granules. The mean quantity of the protein of interest within each of these areas was approximated using the mean fluorescence intensity and standardized to the total fluorescence in the total NK cell. This resulted in the Mean Fluorescence Intensity Ratio used for quantification. For α-tubulin and VASP staining of whole cells to show stability and/or knockdown, mean fluorescence intensity of the entire cell was used. The distance of the MTOC to the synapse and the distance of the individual granules to the MTOC was quantified using the ImageJ length function on images adjusted to increase clarity. To quantify the average distance of the granules to the microtubule-organizing center (MTOC), the distance of each granule to the MTOC was collected. When granules merged, a series of points representing individual granules in size and location was quantified in a grid pattern. The collective granule distances for each cell were averaged to obtain a single value representing the average granule distance in that cell. These average values were then analyzed as a data set. Representative images shown are adjusted to increase clarity of the location of the MTOC and granules.

Statistical analyses were completed using GraphPad Prism version 5.01 software. Most analyses were done using a two-tailed Student's unpaired t-test with comparison of each siRNA treated group to a relevant time matched control siRNA group. A paired Student's t-test was used for assessing perigranular accumulation of 2B4 and VASP, which were costained on the same cells. In the case of the statistical distribution of confocal data (MTOC polarization), a 2-way ANOVA was used to assess the possible differences of percentages across three groups and multiple time points.

Results

VASP knockdown inhibits NK cell cytotoxicity

Mutation in Dedicator of Cytokinesis 8 (DOCK8) is known to cause a complex immunodeficiency resulting in multiple defects in NK cell function (41, 44). In our previous proteomics analysis, numerous actin regulatory proteins, including Wiskott-Aldrich Syndrome protein (WASP) were found in complex with DOCK8 (41). VASP, another actin regulatory protein that is also present in a variety of hematopoietic cell lines including NK cells (Fig. 1A), co-immunoprecipitates with DOCK8 (Fig. 1B, 1C) in the NKL cell line. Interestingly, VASP is seen as a doublet in most cell lines, which likely represents a hyper-phosphorylated form of VASP (45, 46). The association of VASP and DOCK8, paired with the known role of VASP in F-actin polymerization, place VASP in an ideal position to affect NK cell cytotoxicity. On initial observation, the VASP protein present in NKL and primary NK cells appeared mostly at the cytolytic synapse (Fig. 1D, 1G). In order to quantify this relationship, we stained NKL and primary NK cells with a panel of antibodies to define a standard for membrane localized, synapse localized and granule localized proteins (Supplemental Fig. 1A, 1C). This allowed us to observe that NKL and primary NK cell VASP protein associated with the membrane area (Supplemental Fig. 1B, 1D), as well as the synaptic area (Fig. 1E, 1G) in a similar manner to the NK cell receptor 2B4, which is known to localize to the membrane and accumulate at the synapse. Other proteins tested, including

perforin, LAMP-1 and non-specific binding to rIgG can be shown to have a lower synaptic to cell MFI ratio (Fig. 1E, 1G), indicating little to no accumulation in these areas.

In order to determine whether VASP was involved in NK cell-mediated killing, we used two independent short interfering RNAs (siRNA) against VASP that effectively deplete the protein from NKL (Fig. 2A) and primary NK cells (Fig. 2D). Immunoblotting was used to independently verify every VASP knockdown experiment completed. In NKL cells, VASP knockdown resulted in decreased natural cytotoxicity against 721.221 cells (Fig. 2B, 2C). VASP depletion in primary human NK cells also showed decreased natural cytotoxicity against 721.221 (Fig. 2E, 2F) as well as diminished antibody-dependent cytotoxicity through NKG2D and 2B4 (Fig. 2G, 2H) and CD16 (Fig. 2I, 2J). Taken together, these data implicate VASP as a regulator of NK cell-mediated cytotoxicity.

VASP depletion does not impact NK cell conjugate formation or microtubule organizing center polarization

NK cell cytotoxicity proceeds in a series of steps including F-actin generation at the cytolytic synapse, integrin-mediated adhesion, MTOC polarization and lytic granule convergence, any of which could be molecularly disrupted by VASP knockdown. In order to determine where VASP acts to impact NK cell cytotoxicity, we proceeded to interrogate these steps sequentially. To evaluate the accumulation of F-actin at the immunological synapse, NKL (Fig. 3A, 3B) and primary human NK cells were conjugated to CMAC-stained 721.221 cells, stained for F-actin and with anti-VASP antibody and then imaged by confocal microscopy. Where possible, NKL and primary NK cells were additionally stained with an anti-VASP antibody to observe the level of knockdown. Typical examples and quantitation of a single experiment in each NKL (Supplemental Fig. 2A, 2B) and primary NK cells (Supplemental Fig. 2C, 2D) are shown. An additional immunoblot confirmed overall knockdown for each experiment. Unexpectedly, with VASP knockdown, NKL-721.221 conjugates could be formed and visualized – which was unlikely given the default hypothesis that VASP knockdown would affect actin accumulation and dynamic adhesion of NK cells. Surprisingly, NKL cells nucleofected with control siRNA had a similar amount of F-actin accumulation at the synapse to those nucleofected with two independent siRNAs targeting VASP (Fig. 3A, 3B). Primary NK cells showed the same result – where F-actin accumulation at the synapse was unaffected by the loss of VASP (Fig. 3C, 3D). This indicates that, despite its canonical role in F-actin polymerization (11, 13, 24, 26, 47–49), the loss of VASP alone does not appear to impact the ability of NK cells to accumulate F-actin at the cytotoxic synapse.

VASP is also known to orchestrate signaling upstream of integrin activation (27, 34, 50, 51), allowing for activation of the integrin secondary to activation by other cellular receptors. This process allows for the integrin to change into a high affinity conformational state, cluster and to recruit interacting proteins, such as Talin, which allow it to more efficiently bind to its ligand. One such integrin is LFA-1, an important integrin for NK cell-target cell conjugate formation (28–30, 52). Based on this, we assessed the impact of VASP knockdown on the ability of NKL and primary NK cells to accumulate integrin at the CS, and ultimately assessed and quantified their ability to form tight conjugates with 721.221

target cells. To assess the ability of the integrin LFA-1 to accumulate at the synapse, NKL and primary NK cells were stained with anti-LFA-1 and anti-VASP antibody for confocal analysis. As shown in Figure 4A and 4B, knockdown of VASP in NKL cells did not impact the accumulation of LFA-1 at the synapse. A similar result was found for primary NK cells (Fig. 4C, 4D). The distribution of talin, a protein that associates with the extended high-affinity form of LFA-1 (52, 53), was similarly unchanged by VASP knockdown (Fig. 4E, 4F). Additionally, VASP knockdown did not impact the ability of NKL or primary NK cells to form strong conjugates with 721.221 cells (Fig. 4G, 4H). Taken together, these data suggest that initial NK cell synaptic formation does not require VASP.

After formation of a tight synaptic conjugate, the MTOC begins to polarize toward the cytolytic synapse. In order to evaluate the potential role of VASP in this process, NKL and primary NK cells were allowed to form conjugates to CMAC-stained 721.221 cells and were evaluated for the proximity of the MTOC to the synapse by staining for γ-tubulin, a marker of the centrosome. As shown in Figure 5A-C, depletion of VASP using siRNA did not impact the ability of the MTOC to polarize to the synapse, as defined by both the average distance (Fig. 5B, analyzed by Student's t-test) and the statistical distribution of distances between the MTOC and synapse (Fig. 5C, as analyzed by 2-way ANOVA based on histogram shown, $p>0.9999$). Similarly, siRNA-mediated knockdown of VASP in primary NK cells did not impact the proximity of the MTOC to the synapse (Fig. 5D) as determined by both Student's t-test (Fig. 5E) and by analysis of statistical distribution by 2-way ANOVA based on histogram shown (Fig. 5F, $p>0.9999$). These data indicate that MTOC polarization is not dependent on the presence of VASP protein.

VASP is essential for effective lytic granule convergence and localizes within the perigranular area

In order to mediate specific killing, NK cells accumulate lytic granules at the MTOC through minus-end directed movement that involves the dynein/dynactin microtubule motor complex (7). Granule convergence to the MTOC is a crucial step for specificity of cytolysis and to prevent bystander killing (28, 29, 54). Based on this essential step, we assessed the impact of VASP knockdown on the ability of NK cells to effectively converge cytolytic granules to the MTOC. NKL and primary NK cells were allowed to form conjugates with 721.221 target cells for a total of 30 minutes and imaged to determine the location of the MTOC (anti-γ-tubulin) and the cytolytic granules (anti-perforin). In each conjugate, the distance of each individual granule to the MTOC was measured and the average distance of the granules to the MTOC for each conjugate was quantified. Perforin granules generally formed a tight cluster around the MTOC in siCtrl treated NKL, but failed to effectively cluster when VASP was knocked down (Fig. 6A, 6B). In order to determine whether this was a time-dependent relationship, we further quantified the distance of the granule to the MTOC in a time course of six to thirty minutes. As shown in Figure 6C, VASP-depleted NKL cells did not appear to effectively converge their granules at any of the time points analyzed, indicating an overall failure to converge and not a temporal relationship. When analyzed within primary NK cells, a similar defect in granule convergence was observed (Fig. 6E, 6F).

In light of the impact of VASP on granule convergence, we wanted to determine if VASP interacted with the lytic granules strong enough to allow co-purification. Using a previously published lytic granule isolation method (42, 55), which has also been outlined in detail in the methods, we isolated several cellular fractions from NKL cells in order to determine the cellular compartments that contained VASP. As shown in Figure 6G, the crude lysosomal fraction, which includes the cytotoxic granules as indicated by the presence of granzyme B, also contained a quantity of VASP protein. This indicates that VASP co-purifies with the cytolytic granules and lysosomes in the NKL cell line. The quantity seen is admittedly much less than the amount of VASP seen in the other lysates, but considering the large amount of VASP seen at and around the cell membrane, this would generally be expected.

This purification prompted a re-analysis of the previous NKL data (Supplemental Fig. 1A) to determine if any level of VASP could be localized to the perigranular area in these cells. By focusing on the plane with the most granules present within NKL cells conjugated with CMAC-stained 721.221 cells, we were able to observe the amount of immunofluorescence staining present at the granules. As shown in Figure 6H, LAMP-1 and perforin clearly localized to the perigranular area, as their granular mean fluorescence intensity (MFI): whole cell ratio was definitively larger than one. The membrane receptor 2B4, however, did not appear to accumulate at the granules to any level. Although, unsurprisingly, VASP did not accumulate with the granules to the same level as LAMP-1, it did appear to have a granule MFI ratio slightly higher than one. Given the similar membrane localization seen in 2B4, we felt that this served as the best negative control. When comparing these two proteins directly, costained on the same fixed cells, more VASP is present in the perigranular area ($p<0.005$, paired Student's t-test), indicating a positive presence of VASP at the granules.

Given the evidence for the presence of VASP near and around the granules, we wanted to further assess the impact of VASP on the ability of NKL cells to degranulate. To do this, we completed a LAMP-1 externalization assay in the presence of NKL-721.221 conjugates with and without VASP knockdown. As shown in Fig 6J, VASP knockdown showed no impact on the ability of NKL cells to degranulate.

NK cell granule convergence is dependent on VASP-mediated actin accumulation

The presence of VASP at the lytic granule in NKL and primary NK cells could indicate that VASP is affecting granule convergence through action at the granule itself. However, given that the a large amount of VASP protein is located at the immunological synapse in NKL and primary NK cells (Fig. 1E, 1G), and that conjugate formation is required for granule convergence in these models, confounding factors would likely complicate isolation of a role for VASP in lytic granule convergence. Thus, we decided to use a recently described NK cell line, KHYG-1 (56), as a novel model for granule convergence. This cell line, which is derived from an NK cell tumor (56), has been reported to have increased cytotoxicity compared to NKL (57), likely through a constitutive-primed cytolytic state, which allows it to respond faster upon meeting an appropriate target (58). Part of this primed state is the maintenance of cytolytic granules in a converged state, surrounding the MTOC, even before the cells have encountered a target (58). Since this cell line maintains granule convergence

without the formation of an immunological synapse, and localizes a larger portion of cellular VASP with the cytolytic granules (Fig. 7A-D, Supplemental Fig. 3A), it appears to be an optimal model in which to study granule convergence and the impact of granular VASP.

We first assessed whether VASP knockdown in KHYG-1 resulted in the same phenotype as NKL and primary NK cells. Knockdown was assessed across experiments by internal immunofluorescence control, where applicable, and by immunoblot. A representative immunofluorescence image set, experiment and complete experimental findings are shown in Supplemental Fig. 3B-3D respectively. A representative immunoblot is shown in Supplemental Fig. 3E. Knockdown of VASP in KHYG-1 resulted in decreased cytotoxicity against 721.221 target cells (Supplemental Fig. 3F, 3G). In addition, the maintenance of cytotoxic granules in a converged state in KHYG-1 was impaired by the loss of VASP (Fig. 7E, 7F). Similar to NKL, VASP knockdown did not interfere with the ability of KHYG-1 to degranulate when conjugated to CMAC-stained 721.221 target cells (Fig. 7G). Altogether, these data highlight a role for VASP in promoting/maintaining lytic granule convergence to MTOC and a striking similarity between the role of VASP in the NKL and KHYG-1 cell lines.

We next isolated lytic granules from KHYG-1 cells in order to determine which molecular factors were present. This was done in the same manner as described for Fig. 6G, with each subsequent fraction being a subset of the one before it, with the exception of the CLF fraction, which is a subset of the PML. The resulting CLF was used for a resulting immunoprecipitation experiment and subsequently immunoblotted alongside the other logical fractions. The CLF was analyzed for whole contents (marked CLF in Supplemental Fig. 4A), as well as those that co-immunoprecipitated with granule-associated VASP (VASP IP) or rIgG. Similar to in NKL, VASP was present within the crude lysosomal fraction in KHYG-1 (Supplemental Fig. 4A). In addition, we found that VASP could be effectively immunoprecipiated from this fraction, despite a rigorous isolation procedure. Interestingly, WASP, another actin regulatory protein, was present in complex with VASP within the crude lysosomal fraction (Suppl Fig. 4A).

The interaction of two actin regulatory proteins, VASP and WASP and the presence of actin co-purifying with the granules implies that polymerization of F-actin could be occurring at the site of the lytic granule. This is further supported by the presence of F-actin structures near the granule cluster in KHYG-1 cells (Fig. 7A-7D, Supplemental Fig. 3A) and the co-purification of VASP and actin with the crude lysosomal fraction (Supplemental Fig. 4A). Given the known role of VASP in regulating F-actin polymerization, we suspected that VASP might act to enhance F-actin accumulation/stabilization in NK cells. Thus, we decided to test whether actin polymerization itself was needed for the maintenance of converged granules in the KHYG-1 cell line.

The known roles of F-actin in NK cell mediated killing are centered on the synapse, where F-actin is required both for the formation of a stable conjugate with the offending cell and in remodeling to permit the effective delivery of granules to the synapse. Investigations into the role of actin in granule convergence have been limited. One study, published by Mentlik et al, did show no impact of Latrunculin A, an actin depolymerizing agent, on granule

convergence during live cell imaging of YTS cells interacting with 721.221 over a time period of up to 15 minutes (7). The lack of actin polymerization, however, may have had an impact on the cell synapse interactions, resulting in a system where 2 different possible roles of actin cannot be fully delineated. Thus, the KHYG-1 cell line again provides a unique model in which to ascertain the role of F-actin in the maintenance of converged cytolytic granules, without the confounding role that F-actin plays at the synapse. To test this, KHYG-1 cells were treated with 1 μM Latrunculin A to disrupt F-actin filaments. Interestingly, Latrunculin A-treatment mirrored the phenotype seen in VASP knockdown cells, with the lytic granules failing to maintain their convergence at the MTOC (Fig. 7H, 7I). These data suggest that F-actin is involved in lytic granule convergence to the MTOC, and that its accumulation is likely dependent on several known actin regulatory proteins, including VASP.

Actin Polymerization, but not VASP protein, is required for the gross stability of α-tubulin

Minus-end mediated transport on microtubules via dynein is generally thought to be responsible for the convergence of granules to the MTOC (7, 59). One past study previously showed that microtubule destabilization with colcemid caused a similar dispersion of the lytic granules in KHYG-1 (58). Given this known role for microtubules and our finding that VASP is needed for the maintenance of granule convergence, we postulated that an actin-microtubule interaction might be involved, as similar interactions have been seen in other cell systems (60). Given these contributing factors, we hypothesized that VASP might be contributing to an essential stabilizing interaction between the actin and microtubule cytoskeletons. To test this hypothesis, we first assessed the stability of the KHYG-1 microtubule network after treatment with DMSO or Latrunculin A by immunofluorescence images taken in the plane of the MTOC. As shown in Supplemental Fig. 4B, 4C, actin depolymerization by Latrunculin A greatly decreased the detectable mean fluorescence intensity of α-tubulin, while dispersing the granules from the most fluorescent point, presumably the MTOC. This indicates that polymerized actin is required for support of the microtubule network. Given this finding we then interrogated whether VASP knockdown would produce a similar effect. The detectable mean fluorescence intensity of α-tubulin was unchanged in the VASP knockdown cells (Supplemental Fig. 4D, 4E), indicating no gross microtubule destabilization, strikingly dissimilar from the impact seen with Latrunculin A treatment. This indicates that, although VASP, actin polymerization, and microtubule stability all contribute to maintenance of granule convergence, VASP does not appear to affect gross α-tubulin stability in the same manner as actin depolymerization does.

Discussion

Precise reorganization of the NK cell cytoskeleton is instrumental in the NK cell cytolysis and in the release of preformed lytic granules to eliminate target cells. Despite the many essential and well-described functions of the actin and microtubule cytoskeletons in this cytotoxicity, NK cell specific regulation of these proteins is still not well understood. In this study, we describe a specific role for one such actin regulatory protein, VASP, in NK cell mediated cytotoxicity. Specifically, we found that VASP is required for maintenance of cytolytic granule convergence to the MTOC, resulting in more effective cytolysis. We

suspect that this is secondary to VASP's function in promoting actin polymerization, as depolymerization of actin using Latrunculin-A resulted in a similar phenotype. Surprisingly, VASP did not appear to play a dominant role at the NK cell-target cell synapse, where the majority of F-actin polymerization occurs.

VASP has a novel and non-redundant role in NK cell cytotoxicity: VASP maintains converged NK cell lytic granules likely though promotion of actin polymerization. Maintenance of granules in a converged state could represent a secondary process, completely separate or perhaps similar to the active granule convergence, as visualized by live cell imaging. In the active convergence process, the dynein motor complex is thought to drive granule convergence by moving lytic granules along the microtubule network toward the MTOC, with some evidence that this occurs independently of actin polymerization (7). This is in contrast to the maintenance of granule convergence, which we have shown is dependent on actin polymerization. The differences and similarities between these two processes – the initiation of active convergence and the maintenance of the converged state may illuminate several previously unrealized molecular steps to granule convergence. Given that depolymerization of microtubules with colcemid has previously been shown to result in a similar de-convergence of lytic granules in the KHYG-1 cell lines (58), and another microtubule disrupting agent, nocodazole, also prevented granule convergence in live cell imaging of YTS cells (7), microtubule stability appears to be a shared molecular requirement in both active granule convergence and maintenance of granules in a converged state. Our data additionally shows a destabilization of the microtubule cytoskeleton with depolymerization of actin, potentially reflecting a link between these two cytoskeletal requirements. However, this does not explain the reliance on VASP, which did not grossly impact the microtubule arrangement, or if motor proteins, such as dynein, are involved.

In preparations of crude lysosomal fractions, which include the NK cell lytic granules, we found that a small amount of VASP, actin and WASP associated with the granules and that granule-associated WASP could be co-immunoprecipitated with VASP. Although this process does have purification limitations, this circumstantial evidence may indicate highly regulated actin polymerization on or near the granules, as VASP-WASP interactions are linked to F-actin polymerization (12). Interestingly, HkRP3, and WASP also impact NK cell granule convergence (41, 42) and interactions between these proteins may serve as a starting point for understanding the steps of granule convergence. The relationship between actin, VASP and other actin regulatory proteins may represent an opportunity for further understanding of how NK cell lytic granules actively move into and maintain a converged state.

We found that VASP was required for maintenance of granule convergence, but not for degranulation. Although this seems initially counterintuitive, as granule convergence classically precedes degranulation, recent studies (31) have hypothesized that granule convergence may occur independent of activation status and provide a mechanism that allows NK cells to prevent inadvertent release and generally aim. This occurs by moving granules into the interior of the cell, away from precarious positions near the cell membrane. When the decision is made to kill an offending target cell, the granules can be appropriately aimed to minimize bystander damage. However, if granules are spread throughout the cell,

as observed in multiple VASP knockdown NK cell models, random and decentralized degranulation can more easily occur – resulting in inadvertent release, bystander damage and decreased synaptic delivery. When considered in this context, VASP knockdown NK cells could have less productive killing, but quantitatively intact degranulation secondary to ineffective synaptic targeting.

As a member of the Ena/VASP family of actin regulatory proteins, VASP seemed optimally suited for regulating the accumulation and reorganization of F-actin at the NK cell immunological synapse. The gross accumulation of both F-actin and VASP at this location further supported this hypothesis. However, we not only found that VASP knockdown alone does not impact the ability of NK cells to generate F-actin at the cytolytic synapse, but also has no impact on the NK cell-target cell conjugate formation. As LFA-1 is implicated in this granule convergence (31, 32), synaptic VASP could signal downstream of LFA-1 to promote granule convergence,. This possibility, however, is less likely as VASP promotes maintenance of granule convergence even in the absence of a cytotoxic synapse (as seen in the KHYG-1 cell line) or LFA-1 signaling. Another likely possibility is that both EVL and VASP could redundantly promote actin accumulation at the synapse – making VASP expendable at this cellular location.

In all, we show that VASP plays a unique and novel role in lytic granule convergence and that F-actin is critical to maintain converged lytic granules. This previously undescribed requirement for F-actin illuminates new areas for inquiry. In particular, how VASP, actin and microtubules interact, and whether other actin regulatory proteins, such as WASP, are involved. Future studies focusing on F-actin polymerization and regulation should aid in understanding the complex process underlying intracellular lytic granule movement.

Supplementary Material

Refer to Web version on PubMed Central for supplementary material.

Acknowledgments

The authors are grateful to Brittany Overlee and Kenneth Uy for technical assistance. The authors are also appreciative of the members of the Billadeau laboratory for helpful discussions.

This work was supported by the Mayo Foundation and National Institute of Allergy and Infectious Diseases Grant R01-AI120949 (to D.D.B.). KMW was supported by the National Institutes of General Medical Sciences (grant T32-GM-65841) and the Mayo Clinic College of Medicine's Medical Scientist Training Program.

Abbreviations used in this article:

APC	Allophycocyanin
$CaCl_2$	Calcium Chloride Isolation Fraction
CLF	Crude Lysosomal fraction
CMAC	7-amino-4-chloromethylcoumarin
CS	cytotoxic synapse

DMSO	Dimethyl sulfoxide
DOCK8	Dedicator of Cytokinesis 8
Ena	Enabled
E:T ratio	Effector to target ratio
EVH1	Ena/VASP Homology 1
EVH2	Ena/VASP Homology 2
Evl	Ena/VASP Like
F-actin	Filamentous actin
FITC	Fluorescein isothiocanate
GST	glutathione S-transferase
HkRP3	Hook-related protein 3
IS	Immunological synapse
kD	kilodalton
Lat A	Latrunculin A
LFA-1	lymphocyte function-associated antigen 1
MFI	Mean Fluorescence Intensity
MTOC	microtubule organizing center
NK cell	Natural killer cells
PBMC	Peripheral Blood Mononuclear Cell
PBS	Phosphate Buffered Saline
PE	R-phycoerythrin
PerCP	Peridinin-Chlorophyll-protein
PLL	poly-L-lysine
PML	Post Mitochondrial Lysate
PNL	Post Nuclear Lysate
rIgG	rabbit Immunoglobulin G
Rpm	rotations per minute
RPMI	Roswell park Memorial Institute Media
SH3	Src Homology 3

siRNA	small interfering RNA
VASP	Vasodialator Stimulated Phosphoprotein
WCL	whole cell lysate
WASP	Wiskott Aldrich Syndrome Protein
WIP	WASP Interacting Protein
WW	rsp5-domain or WWP repeating motif

References

1. Bakker AB, Wu J, Phillips JH, and Lanier LL 2000 NK cell activation: distinct stimulatory pathways counterbalancing inhibitory signals. Hum Immunol 61: 18–27. [PubMed: 10658974]
2. Biassoni R 2008 Natural killer cell receptors. Adv Exp Med Biol 640: 35–52. [PubMed: 19065782]
3. Brumbaugh KM, Binstadt BA, and Leibson PJ 1998 Signal transduction during NK cell activation: balancing opposing forces. Curr Top Microbiol Immunol 230: 103–122. [PubMed: 9586353]
4. Lanier LL 2003 Natural killer cell receptor signaling. Curr Opin Immunol 15: 308–314. [PubMed: 12787756]
5. Lagrue K, Carisey A, Oszmiana A, Kennedy PR, Williamson DJ, Cartwright A, Barthen C, and Davis DM 2013 The central role of the cytoskeleton in mechanisms and functions of the NK cell immune synapse. Immunol Rev 256: 203–221. [PubMed: 24117823]
6. Mace EM, Dongre P, Hsu HT, Sinha P, James AM, Mann SS, Forbes LR, Watkin LB, and Orange JS 2014 Cell biological steps and checkpoints in accessing NK cell cytotoxicity. Immunol Cell Biol 92: 245–255. [PubMed: 24445602]
7. Mentlik AN, Sanborn KB, Holzbaur EL, and Orange JS 2010 Rapid lytic granule convergence to the MTOC in natural killer cells is dependent on dynein but not cytolytic commitment. Mol Biol Cell 21: 2241–2256. [PubMed: 20444980]
8. Barzik M, Kotova TI, Higgs HN, Hazelwood L, Hanein D, Gertler FB, and Schafer DA 2005 Ena/VASP proteins enhance actin polymerization in the presence of barbed end capping proteins. J Biol Chem 280: 28653–28662. [PubMed: 15939738]
9. Bear JE, Svitkina TM, Krause M, Schafer DA, Loureiro JJ, Strasser GA, Maly IV, Chaga OY, Cooper JA, Borisy GG, and Gertler FB 2002 Antagonism between Ena/VASP proteins and actin filament capping regulates fibroblast motility. Cell 109: 509–521. [PubMed: 12086607]
10. Benz PM, Blume C, Seifert S, Wilhelm S, Waschke J, Schuh K, Gertler F, Munzel T, and Renne T 2009 Differential VASP phosphorylation controls remodeling of the actin cytoskeleton. J Cell Sci 122: 3954–3965. [PubMed: 19825941]
11. Breitsprecher D, Kiesewetter AK, Linkner J, Vinzenz M, Stradal TE, Small JV, Curth U, Dickinson RB, and Faix J 2011 Molecular mechanism of Ena/VASP-mediated actin-filament elongation. EMBO J 30: 456–467. [PubMed: 21217643]
12. Castellano F, Le Clainche C, Patin D, Carlier MF, and Chavrier P 2001 A WASp-VASP complex regulates actin polymerization at the plasma membrane. EMBO J 20: 5603–5614. [PubMed: 11598004]
13. Chen XJ, Squarr AJ, Stephan R, Chen B, Higgins TE, Barry DJ, Martin MC, Rosen MK, Bogdan S, and Way M 2014 Ena/VASP proteins cooperate with the WAVE complex to regulate the actin cytoskeleton. Dev Cell 30: 569–584. [PubMed: 25203209]
14. Kim HR, Graceffa P, Ferron F, Gallant C, Boczkowska M, Dominguez R, and Morgan KG 2010 Actin polymerization in differentiated vascular smooth muscle cells requires vasodilator-stimulated phosphoprotein. Am J Physiol Cell Physiol 298: C559–571. [PubMed: 20018948]
15. Laurent V, Loisel TP, Harbeck B, Wehman A, Grobe L, Jockusch BM, Wehland J, Gertler FB, and Carlier MF 1999 Role of proteins of the Ena/VASP family in actin-based motility of Listeria monocytogenes. J Cell Biol 144: 1245–1258. [PubMed: 10087267]

16. Lin WH, Nebhan CA, Anderson BR, and Webb DJ 2010 Vasodilator-stimulated phosphoprotein (VASP) induces actin assembly in dendritic spines to promote their development and potentiate synaptic strength. J Biol Chem 285: 36010–36020. [PubMed: 20826790]
17. Meyer G, and Feldman EL 2002 Signaling mechanisms that regulate actin-based motility processes in the nervous system. J Neurochem 83: 490–503. [PubMed: 12390511]
18. Plastino J, Olivier S, and Sykes C 2004 Actin filaments align into hollow comets for rapid VASP-mediated propulsion. Curr Biol 14: 1766–1771. [PubMed: 15458649]
19. Siton O, and Bernheim-Groswasser A 2014 Reconstitution of actin-based motility by vasodilator-stimulated phosphoprotein (VASP) depends on the recruitment of F-actin seeds from the solution produced by cofilin. J Biol Chem 289: 31274–31286. [PubMed: 25246528]
20. Trichet L, Campas O, Sykes C, and Plastino J 2007 VASP governs actin dynamics by modulating filament anchoring. Biophys J 92: 1081–1089. [PubMed: 17098798]
21. Wu Y, and Gunst SJ 2015 Vasodilator-stimulated phosphoprotein (VASP) regulates actin polymerization and contraction in airway smooth muscle by a vinculin-dependent mechanism. J Biol Chem 290: 11403–11416. [PubMed: 25759389]
22. Bachmann C, Fischer L, Walter U, and Reinhard M 1999 The EVH2 domain of the vasodilator-stimulated phosphoprotein mediates tetramerization, F-actin binding, and actin bundle formation. J Biol Chem 274: 23549–23557. [PubMed: 10438535]
23. Edwards M, Zwolak A, Schafer DA, Sept D, Dominguez R, and Cooper JA 2014 Capping protein regulators fine-tune actin assembly dynamics. Nat Rev Mol Cell Biol 15: 677–689. [PubMed: 25207437]
24. Pasic L, Kotova T, and Schafer DA 2008 Ena/VASP proteins capture actin filament barbed ends. J Biol Chem 283: 9814–9819. [PubMed: 18283104]
25. Sechi AS, and Wehland J 2004 ENA/VASP proteins: multifunctional regulators of actin cytoskeleton dynamics. Front Biosci 9: 1294–1310. [PubMed: 14977545]
26. Chereau D, and Dominguez R 2006 Understanding the role of the G-actin-binding domain of Ena/VASP in actin assembly. J Struct Biol 155: 195–201. [PubMed: 16684607]
27. Deevi RK, Koney-Dash M, Kissenpfennig A, Johnston JA, Schuh K, Walter U, and Dib K 2010 Vasodilator-stimulated phosphoprotein regulates inside-out signaling of beta2 integrins in neutrophils. J Immunol 184: 6575–6584. [PubMed: 20483741]
28. Gross CC, Brzostowski JA, Liu D, and Long EO 2010 Tethering of intercellular adhesion molecule on target cells is required for LFA-1-dependent NK cell adhesion and granule polarization. J Immunol 185: 2918–2926. [PubMed: 20675589]
29. Barber DF, Faure M, and Long EO 2004 LFA-1 contributes an early signal for NK cell cytotoxicity. J Immunol 173: 3653–3659. [PubMed: 15356110]
30. Hildreth JE, Gotch FM, Hildreth PD, and McMichael AJ 1983 A human lymphocyte-associated antigen involved in cell-mediated lympholysis. Eur J Immunol 13: 202–208. [PubMed: 6339253]
31. Hsu HT, Mace EM, Carisey AF, Viswanath DI, Christakou AE, Wiklund M, Onfelt B, and Orange JS 2016 NK cells converge lytic granules to promote cytotoxicity and prevent bystander killing. J Cell Biol 215: 875–889. [PubMed: 27903610]
32. Hsu HT, and Orange JS 2014 Distinct integrin-dependent signals define requirements for lytic granule convergence and polarization in natural killer cells. Sci Signal 7: pe24. [PubMed: 25292212]
33. Maruoka M, Sato M, Yuan Y, Ichiba M, Fujii R, Ogawa T, Ishida-Kitagawa N, Takeya T, and Watanabe N 2012 Abl-1-bridged tyrosine phosphorylation of VASP by Abelson kinase impairs association of VASP to focal adhesions and regulates leukaemic cell adhesion. Biochem J 441: 889–899. [PubMed: 22014333]
34. Estin ML, Thompson SB, Traxinger B, Fisher MH, Friedman RS, and Jacobelli J 2017 Ena/VASP proteins regulate activated T-cell trafficking by promoting diapedesis during transendothelial migration. Proc Natl Acad Sci U S A 114: E2901–E2910. [PubMed: 28320969]
35. Krause M, Sechi AS, Konradt M, Monner D, Gertler FB, and Wehland J 2000 Fyn-binding protein (Fyb)/SLP-76-associated protein (SLAP), Ena/vasodilator-stimulated phosphoprotein (VASP) proteins and the Arp2/3 complex link T cell receptor (TCR) signaling to the actin cytoskeleton. J Cell Biol 149: 181–194. [PubMed: 10747096]

36. Phatarpekar PV, Lee DA, and Somanchi SS 2016 Electroporation of siRNA to Silence Gene Expression in Primary NK Cells. Methods Mol Biol 1441: 267–276. [PubMed: 27177673]
37. Gomez TS, Kumar K, Medeiros RB, Shimizu Y, Leibson PJ, and Billadeau DD 2007 Formins regulate the actin-related protein 2/3 complex-independent polarization of the centrosome to the immunological synapse. Immunity 26: 177–190. [PubMed: 17306570]
38. Savoy DN, Billadeau DD, and Leibson PJ 2000 Cutting edge: WIP, a binding partner for Wiskott-Aldrich syndrome protein, cooperates with Vav in the regulation of T cell activation. J Immunol 164: 2866–2870. [PubMed: 10706671]
39. Banerjee PP, Pandey R, Zheng R, Suhoski MM, Monaco-Shawver L, and Orange JS 2007 Cdc42-interacting protein-4 functionally links actin and microtubule networks at the cytolytic NK cell immunological synapse. J Exp Med 204: 2305–2320. [PubMed: 17785506]
40. Maasho K, Marusina A, Reynolds NM, Coligan JE, and Borrego F 2004 Efficient gene transfer into the human natural killer cell line, NKL, using the Amaxa nucleofection system. J Immunol Methods 284: 133–140. [PubMed: 14736423]
41. Ham H, Guerrier S, Kim J, Schoon RA, Anderson EL, Hamann MJ, Lou Z, and Billadeau DD 2013 Dedicator of cytokinesis 8 interacts with talin and Wiskott-Aldrich syndrome protein to regulate NK cell cytotoxicity. J Immunol 190: 3661–3669. [PubMed: 23455509]
42. Ham H, Huynh W, Schoon RA, Vale RD, and Billadeau DD 2015 HkRP3 is a microtubule-binding protein regulating lytic granule clustering and NK cell killing. J Immunol 194: 3984–3996. [PubMed: 25762780]
43. Gomez TS, Hamann MJ, McCarney S, Savoy DN, Lubking CM, Heldebrant MP, Labno CM, McKean DJ, McNiven MA, Burkhardt JK, and Billadeau DD 2005 Dynamin 2 regulates T cell activation by controlling actin polymerization at the immunological synapse. Nat Immunol 6: 261–270. [PubMed: 15696170]
44. Mizesko MC, Banerjee PP, Monaco-Shawver L, Mace EM, Bernal WE, Sawalle-Belohradsky J, Belohradsky BH, Heinz V, Freeman AF, Sullivan KE, Holland SM, Torgerson TR, Al-Herz W, Chou J, Hanson IC, Albert MH, Geha RS, Renner ED, and Orange JS 2013 Defective actin accumulation impairs human natural killer cell function in patients with dedicator of cytokinesis 8 deficiency. J Allergy Clin Immunol 131: 840–848. [PubMed: 23380217]
45. Halbrugge M, Friedrich C, Eigenthaler M, Schanzenbacher P, and Walter U 1990 Stoichiometric and reversible phosphorylation of a 46-kDa protein in human platelets in response to cGMP- and cAMP-elevating vasodilators. J Biol Chem 265: 3088–3093. [PubMed: 2154470]
46. Halbrugge M, and Walter U 1989 Purification of a vasodilator-regulated phosphoprotein from human platelets. Eur J Biochem 185: 41–50. [PubMed: 2806262]
47. Hansen SD, and Mullins RD 2010 VASP is a processive actin polymerase that requires monomeric actin for barbed end association. J Cell Biol 191: 571–584. [PubMed: 21041447]
48. Krause M, Dent EW, Bear JE, Loureiro JJ, and Gertler FB 2003 Ena/VASP proteins: regulators of the actin cytoskeleton and cell migration. Annu Rev Cell Dev Biol 19: 541–564. [PubMed: 14570581]
49. Kwiatkowski AV, Gertler FB, and Loureiro JJ 2003 Function and regulation of Ena/VASP proteins. Trends Cell Biol 13: 386–392. [PubMed: 12837609]
50. Kwon HW, Shin JH, Cho HJ, Rhee MH, and Park HJ 2016 Total saponin from Korean Red Ginseng inhibits binding of adhesive proteins to glycoprotein IIb/IIIa via phosphorylation of VASP (Ser(157)) and dephosphorylation of PI3K and Akt. J Ginseng Res 40: 76–85. [PubMed: 26843825]
51. Thom SR, Bhopale VM, Yang M, Bogush M, Huang S, and Milovanova TN 2011 Neutrophil beta2 integrin inhibition by enhanced interactions of vasodilator-stimulated phosphoprotein with S-nitrosylated actin. J Biol Chem 286: 32854–32865. [PubMed: 21795685]
52. Mace EM, Zhang J, Siminovitch KA, and Takei F 2010 Elucidation of the integrin LFA-1-mediated signaling pathway of actin polarization in natural killer cells. Blood 116: 1272–1279. [PubMed: 20472831]
53. Mace EM, Monkley SJ, Critchley DR, and Takei F 2009 A dual role for talin in NK cell cytotoxicity: activation of LFA-1-mediated cell adhesion and polarization of NK cells. J Immunol 182: 948–956. [PubMed: 19124737]

54. Zhang M, March ME, Lane WS, and Long EO 2014 A signaling network stimulated by beta2 integrin promotes the polarization of lytic granules in cytotoxic cells. Sci Signal 7: ra96. [PubMed: 25292215]

55. Schenkman JB, and Cinti DL 1978 Preparation of microsomes with calcium. Methods Enzymol 52: 83–89. [PubMed: 672658]

56. Yagita M, Huang CL, Umehara H, Matsuo Y, Tabata R, Miyake M, Konaka Y, and Takatsuki K 2000 A novel natural killer cell line (KHYG-1) from a patient with aggressive natural killer cell leukemia carrying a p53 point mutation. Leukemia 14: 922–930. [PubMed: 10803526]

57. Suck G, Branch DR, Smyth MJ, Miller RG, Vergidis J, Fahim S, and Keating A 2005 KHYG-1, a model for the study of enhanced natural killer cell cytotoxicity. Exp Hematol 33: 1160–1171. [PubMed: 16219538]

58. Suck G, Branch DR, Aravena P, Mathieson M, Helke S, and Keating A 2006 Constitutively polarized granules prime KHYG-1 NK cells. Int Immunol 18: 1347–1354. [PubMed: 16849396]

59. James AM, Hsu HT, Dongre P, Uzel G, Mace EM, Banerjee PP, and Orange JS 2013 Rapid activation receptor- or IL-2-induced lytic granule convergence in human natural killer cells requires Src, but not downstream signaling. Blood 121: 2627–2637. [PubMed: 23380740]

60. Aspengren S, Wielbass L, and Wallin M 2006 Effects of acrylamide, latrunculin, and nocodazole on intracellular transport and cytoskeletal organization in melanophores. Cell Motil Cytoskeleton 63: 423–436. [PubMed: 16671098]

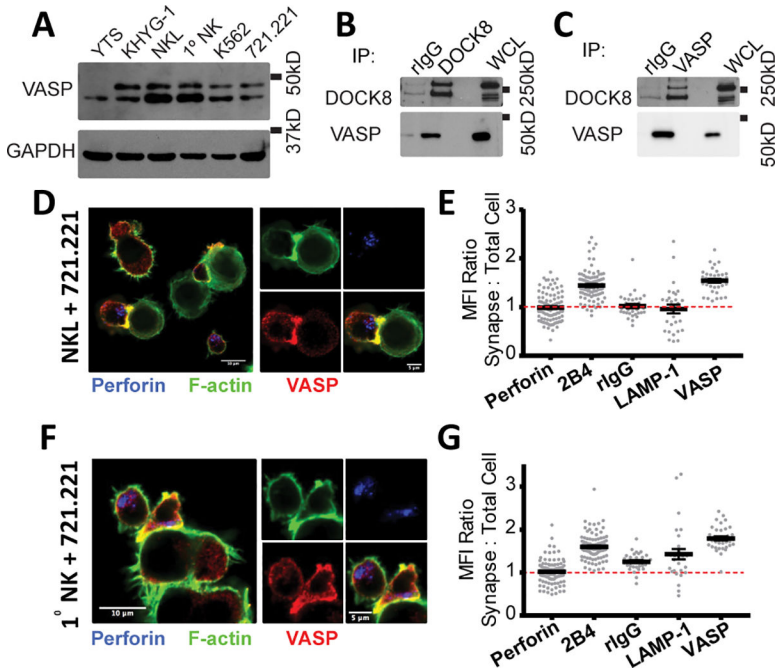

FIGURE 1.

VASP localizes to the immunological synapse and granules in NK cells. (**A)** Whole-cell lysates from the panel of cell lines indicated were immunoblotted for VASP and GAPDH. **(B)** DOCK8 and **(C)** VASP protein were immunoprecipitated from NKL lysates and immunoblotted for the presence of DOCK8 and VASP. Representative immunofluorescence images of NKL-721.221 (**D**) and primary NK-721.221 (**F**) conjugates stained for VASP (red), perforin (blue) and F-actin (green). Quantitation of the Mean Fluorescence Intensity (MFI) of various proteins and rIgG at the cytotoxic synapse in comparison to the MFI of the entire NKL (**E**) or primary NK cell (**G**). All results are representative of at least three independent experiments.

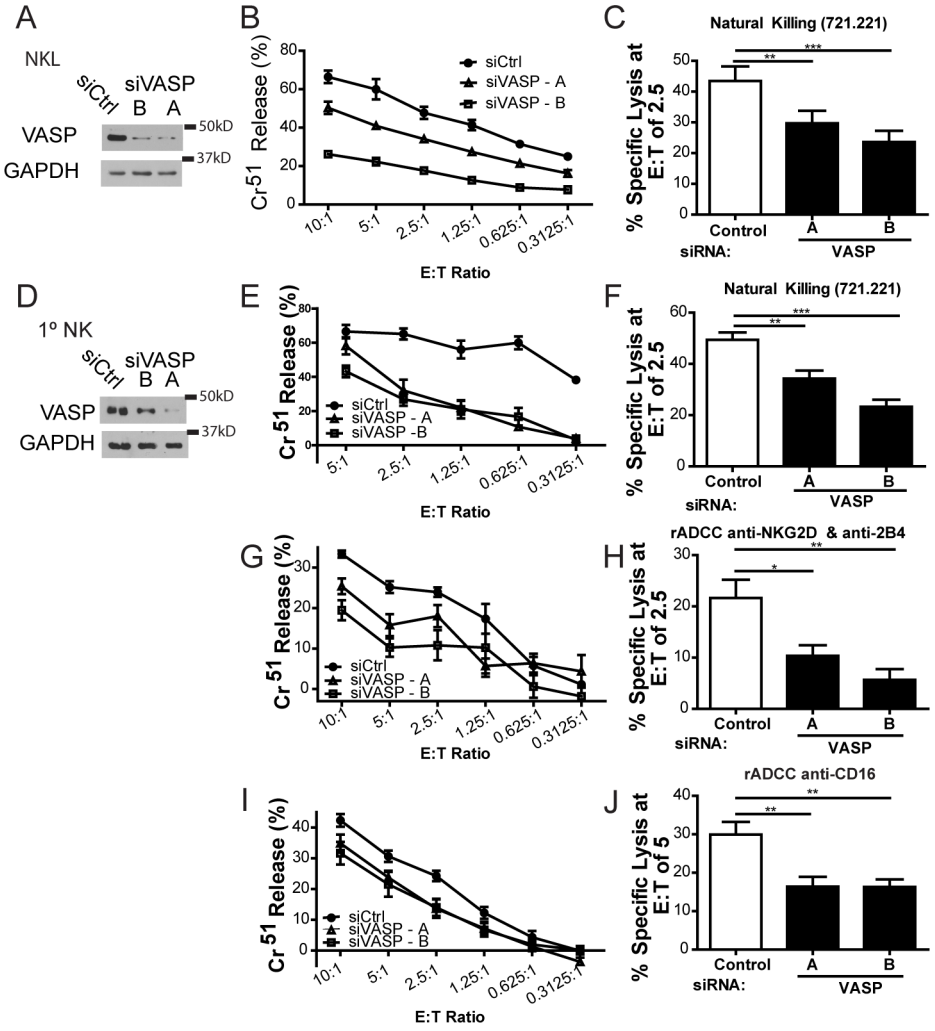

FIGURE 2.

VASP contributes to NK cell cytotoxicity. NKL (**A-C**) and primary NK (**D-J**) cells were nucleofected with control siRNA (siCtrl) or one of two siRNAs targeting VASP. Immunoblot is cropped for clarity. (**A**,**D**) Seventy-two hours after nucleofection, levels of VASP protein were assessed by immunoblot for each experiment. (**B**, **E**) Nucleofected cells were incubated at 37°C for three hours with ^{51}Cr-labeled 721.221 cells at the indicated effector to target (E:T) ratios and specific lysis was calculated. (**C**, **F**) Results were quantified for an E;T ratio of 2.5 effectors to one target cell over six independent experiments. (**G**, **I**) Primary NK cells were incubated with ^{51}Cr-labeled p815 cells coated with either anti-NKG2D + anti-2B4, or with anti-CD16. Percent specific lysis was calculated. (**H**, **J**) Results were quantified at an E:T ratio of 5 (anti-CD16) or 2.5 (anti-NKG2D + anti-2B4) over four independent experiments. All experiments were completed in triplicate or quadruplicate and in reference to spontaneous and total lysis. Results show representative experiments (center and left; **A**, **B**, **D**, **E**, **G**, **I**) or average values over multiple experiments (right; **C**, **F**, **H**, **J**). Error bars indicate SEM. *p < 0.05, ** p < 0.005, and ***p < 0.0005 compared with control group.

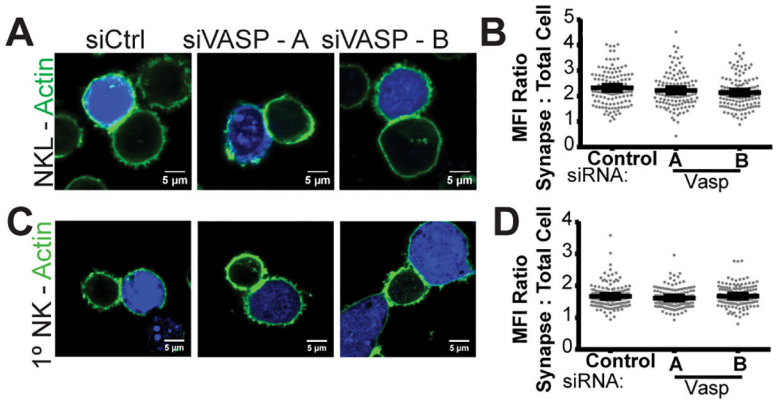

FIGURE 3.

VASP knockdown does not impact gross actin accumulation at the immunological synapse. NKL (**A**-**B**) and primary NK (**C**-**D**) cells were nucleofected with control siRNA (siCtrl) or one of two siRNAs targeting VASP. After seventy-hours NKL and primary NK cells were allowed to form conjugates with7-amino-4-chloromethylcoumarin (CMAC)-labelled 721.221 cells (blue) at 37°C and imaged for the location of F-actin (green) within the NKL or primary NK cell. Thirty to fifty cells in each group were imaged in each of three or four independent experiments. Representative examples (**A**, **C**) and quantitation of synaptic actin fluorescence relative to cellular actin fluorescence and synapse size (**B**, **D**) are shown. Error bars indicate SEM. *$p < 0.05$ compared with control group.

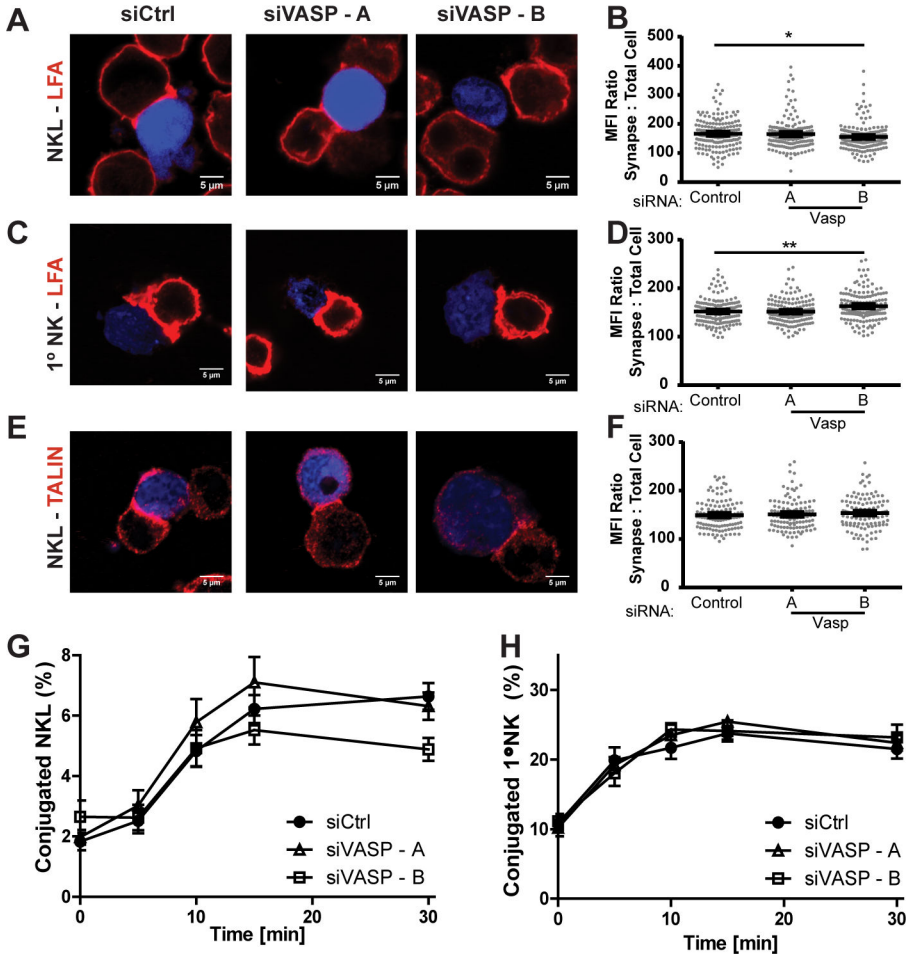

FIGURE 4.

VASP does not impact NK cell conjugate formation. NKL and primary NK cells were nucleofected with control or two siRNAs targeting VASP. (**A-F**) Seventy two hours after nucleofection, NKL and primary NK cells were allowed to form conjugates with CMAC-stained 721.221 cells (blue) at 37° and imaged for the localization of LFA-1 or talin, as indicated. (**B**, **D**, **F**) The amount of synaptic LFA-1 or talin was quantified in relation to the amount of cellular protein and the size of the synapse, as described in the methods. Results were quantified for thirty to fifty conjugates per group for each of three independent experiments for each finding. (**G**, **H**) 72 hours after nucleofection, NKL and primary NK cells stained with Calcein-AM and then allowed to form conjugates at 37°C with CMAC-labeled 721.221 cells over the specified times and then fixed. The formation of conjugates (CMAC + Calcein-AM+) in respect to the total number of NK / NKL cells (Calcein-AM+) was assessed using two color flow cytometry. Results shown are the average of 5 (primary NK) or 7 (NKL) replicate experiments, each performed in triplicate. Error bars indicate SEM. *p < 0.05, ** $p < 0.005$, and ***p < 0.0005 compared with control group.

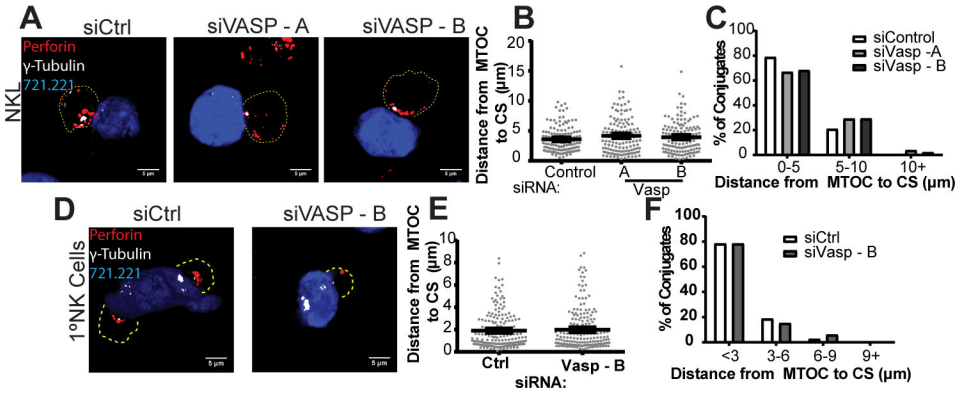

FIGURE 5.

VASP does not impact MTOC Polarization to the NK cell Cytotoxic Synapse (CS). NKL and primary NK cells were nucleofected with control siRNA (siCtrl) or one of two siRNAs targeting VASP. Seventy-two hours after nucleofection, NKL / primary NK cells were incubated at 37°C to allow conjugation with CMAC-stained 721.221 cells (blue). Cells were fixed and imaged for the location of the MTOC (γ-Tubulin, white) and the location of the lytic granules (perforin, red). The periphery of the cells, as defined by F-actin staining, and is designated by a dotted line. All measurements were measured as the distance between the γ-tubulin location within the NKL / primary NK cell, and the nearest point of synapse with the CMAC stain. (**A**) Representative example of NKL conjugates allowed to form for thirty minutes and (**B**, **C**) quantified for three independent experiments of thirty to fifty conjugates per group per experiment. (**D**) Representative example of Primary NK cell conjugates allowed to form for thirty minutes and (**E**, **F**) quantified for three independent experiments of thirty to fifty conjugates per group per experiment. Error bars indicate SEM. *p < 0.05, ** *p* < 0.005, and ***p < 0.0005 compared with control group.

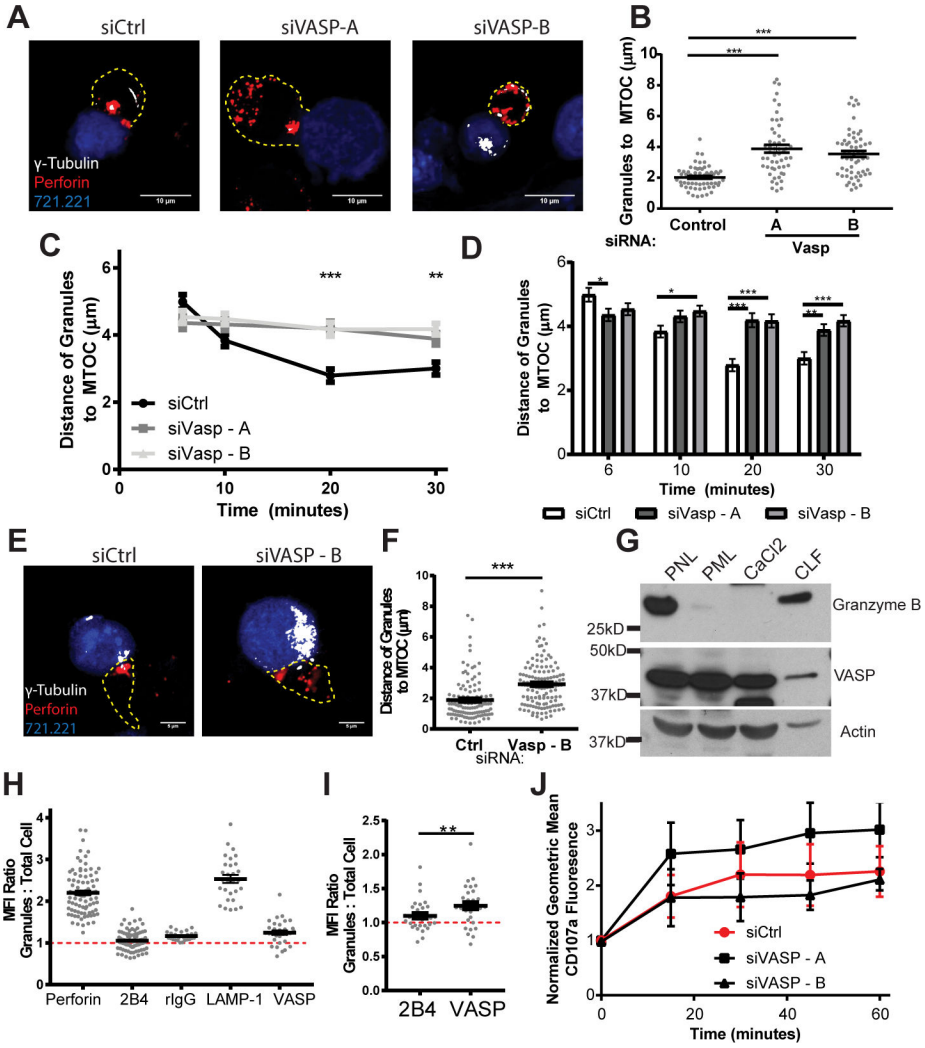

FIGURE 6.

VASP aids lytic granule convergence to the MTOC and co-purifies with lytic granules. NKL and primary NK cells were nucleofected with control siRNA (siCtrl) or one of two siRNAs targeting VASP. Seventy-two hours after nucleofection, NKL / primary NK cells were incubated at 37°C to allow conjugation with CMAC-stained 721.221 cells (blue). Cells were fixed and imaged for the location of the MTOC (γ-Tubulin, white) and the location of the lytic granules (via perforin, red). The periphery of the cells, as defined by F-actin staining, is designated by a dotted line. All measurements were measured as the average distance between all of the perforin granules (red) within the NKL or primary NK cell and the location of the MTOC marked by γ-tubulin. Details are described within the methods section. (**A**) Representative example of NKL conjugates allowed to form for thirty minutes and (**B**) quantified for three independent experiments of thirty to fifty conjugates per group per experiment. (**C**, **D**) NKL Conjugates were allowed to form for six, ten, twenty and thirty minutes and evaluated for the distance of the lytic granules from the MTOC. (**E**) Representative example of Primary NK cell conjugates allowed to form for thirty minutes and (**F**) quantified for three independent experiments of thirty to fifty conjugates per group

per experiment. (**G**) Post nuclear, post mitochondrial, $CaCl_2$ and crude lysosomal fractions were isolated from unstimulated NKL cells as described previously(42), and immunoblotted as indicated. Immunoblot is representative of three independent experiments. (**H**) Conjugates of NKL and CMAC-stained 721.221 cells were imaged in the plane with the most granules and evaluated for the mean fluorescence intensity (MFI) of each of the indicated proteins in the perigranular area in relation to the total cellular MFI. (**I**) Direct analysis of the difference in granular MFI ratios between the two proteins known to the highly membrane localized: 2B4 and VASP. (**J**) CMAC-stained 721.221 target cells and Calcein-AM stained NKL were allowed to form conjugates over the designated time course and then assessed by flow cytometry for the externalization of CD107a / LAMP-1. Results for each experimental group were normalized to their initial Geometric MFI at time zero. Results shown are the analysis of 3 independent experiments each completed in triplicate. Error bars indicate SEM. *$p < 0.05$, ** $p < 0.005$, and ***$p < 0.0005$ compared with control group.

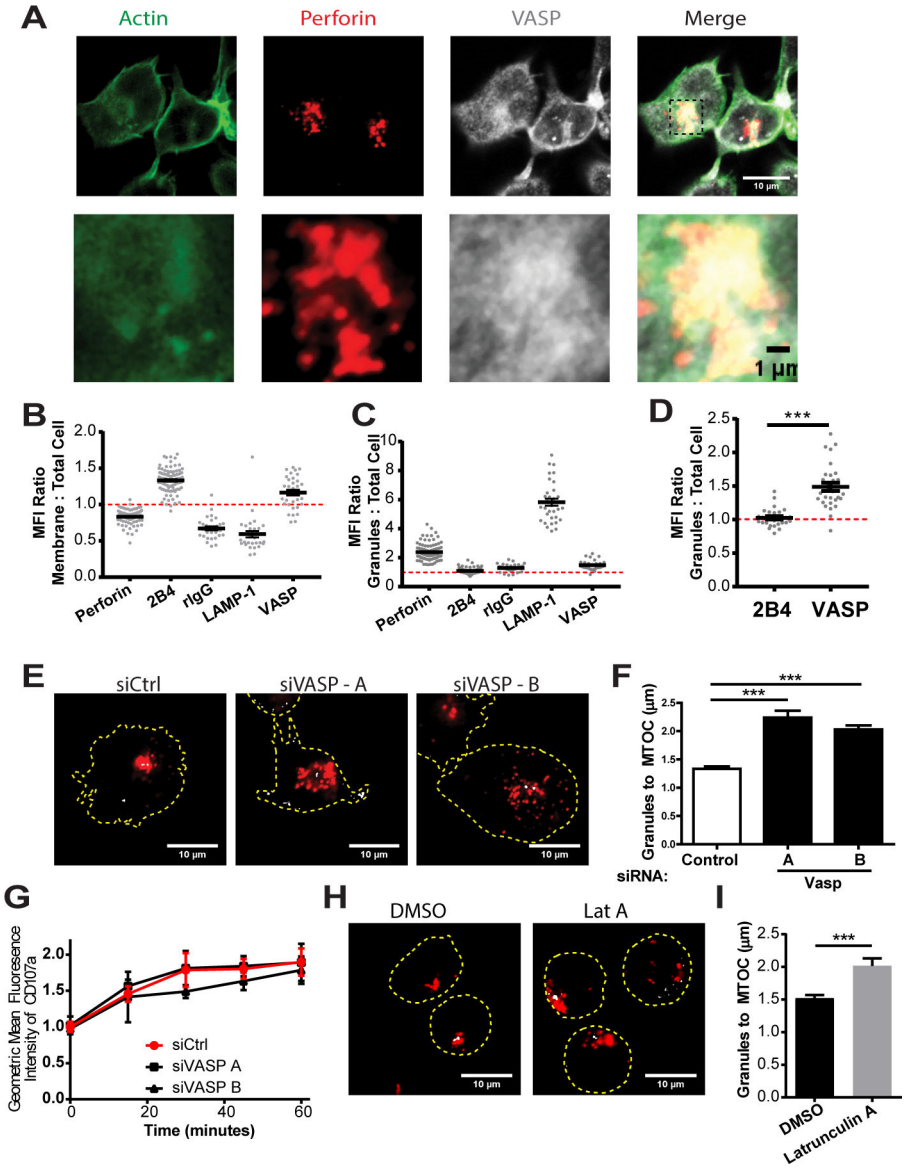

FIGURE 7.

Constitutive granule polarization in KHYG-1 is dependent on VASP and F-actin polymerization. (**A**) KHYG-1 cells were incubated for fifteen minutes at 37°C on PLL-coated coverslips, fixed and then imaged for the location of perforin (to indicate the location of the lytic granules) and VASP. Quantification of the MFI enhancement of the indicated proteins at the (**B**) membrane and (**C**) granules by immunofluorescence. (**D**) Specific analysis of the difference in granule MFI to cell MFI ratios of the two membrane localized proteins is specifically shown on a separate scale. (**E**) KHYG-1 cells nucleofected with control siRNA, or VASP targeting siRNA were allowed to adhere to PLL-coated coverslips for fifteen minutes, fixed and imaged for the location of perforin (red), and γ-tubulin (grey). Representative images are shown. (**F**) Three independent experiments, each including thirty to fifty images were quantified for the average distance for each cell between the perforin granules and the MTOC. (**G**) KHYG-1 cells were allowed to form conjugates with 721.221

cells and the Mean Fluorescence Intensity (MFI) of LAMP-1 / CD107a was assessed on only those NKL conjugated with 721.221 cells over the indicated timecourse. (**H**) KHYG-1 cells were treated with Latrunculin A for ten minutes and then allowed to adhere to PLL-coated coverslips for five minutes before fixation and staining for perforin (red) and γ-tubulin (grey). (**I**) The average distance between the perforin granules and the MTOC for each cell was quantified. Results include three independent experiments, each including thirty to fifty cells per group. Error bars indicate SEM. *p < 0.05, ** $p < 0.005$, and ***p < 0.0005 compared with control group.